JOURNAL OF SPACECRAFT AND ROCKETS
Vol. 35, No. 2, March–April 1998

Trajectory Design in the Sun–Earth–Moon System Using Lunar Gravity Assists

Roby S. Wilson* and Kathleen C. Howell†
Purdue University, West Lafayette, Indiana 47907-1282

The objective of this work is the development of efficient techniques for the preliminary design of trajectories that encounter the moon and must satisfy specific trajectory requirements, such as apogee placement, launch constraints, or end-state targeting. These types of trajectories are highly applicable to mission design in the restricted three- and four-body problems. The general solution approach proceeds in three steps. In the initial analysis, conic arcs and/or other types of trajectory segments are connected at patch points to construct a first approximation. Next, multiconic methods are used to incorporate any additional force model effects that may have been neglected in the initial analysis. An optimization procedure is then employed to reduce the effective velocity discontinuities while satisfying any constraints. Finally, a numerical differential corrections process results in a fully continuous multiple-lunar-swingby trajectory that satisfies the constraints and includes appropriate lunar and solar gravitational models.

Nomenclature

A, B, C, D	= submatrices of the state transition matrix
a	= semimajor axis
C_i	= conic endpoint
e	= eccentricity
$G \cdot M^*$	= dimensional gravitational parameter, 403,503 km^3/s^2
i	= inclination
JD	= Julian date
L_i	= libration point
L^*	= dimensional length, 384,388 km
M	= state relationship matrix
N_{apos}	= number of apogees
N_{mos}	= number of months
P, A	= perigee, apogee
R_E	= Earth radius, 6378.14 km
R_p	= perigee radius
$\boldsymbol{R}, \boldsymbol{V}, \boldsymbol{a}$	= position, velocity, and acceleration vectors
T^*	= dimensional time, 375,173 s
t	= time
$\hat{\boldsymbol{X}}, \hat{\boldsymbol{Y}}, \hat{\boldsymbol{Z}}$	= inertial unit vectors
$\hat{\boldsymbol{x}}, \hat{\boldsymbol{y}}, \hat{\boldsymbol{z}}$	= rotating unit vectors
α_k	= constraint k
$\Delta \boldsymbol{V}$	= velocity discontinuity vector
θ	= true anomaly
ξ, η	= conic parameterizations
$\sigma_{0,1,2}$	= set of switching parameters
Φ	= state transition matrix
χ, ψ	= phasing angles
Ω	= ascending node

Introduction

THE goal of this study is the development of a design tool to create multiple-lunar-swingby trajectories in an efficient and accurate manner and one that is applicable for a variety of mission scenarios. The examples in this paper demonstrate two such possible trajectory concepts. The first example focuses on using multiple lunar gravity assists to achieve a fixed line of apsides with respect to the sun–Earth line. The second type uses a single gravity assist to insert into an orbit in the vicinity of one of the sun–Earth libration points.

In this analysis, the problem solution is separated into a sequence of increasingly complex steps.[1,2] Initially, the trajectory is approximated as a series of geocentric arcs that encounter the moon at the beginning and/or end of each leg. This analysis is useful in establishing general trajectory characteristics such as orientation relative to the sun, apogee distances, and approximate lunar encounter times.[3,4] Note that, although these arcs are frequently assumed to be conics, it is also possible to employ other types of approximate trajectory arcs to obtain this initial solution. For example, solutions of a restricted three-body (or four-body) problem can be used to obtain an initial approximation for transfers from Earth to the sun–Earth libration points.[5] In the next step of the process, the initial approximation is improved by using multiconic techniques to incorporate the effects of additional gravity fields, with the goal of preserving the general characteristics of the initial approximate trajectory. (These multiconic techniques are not limited to gravitational perturbations but can also be used to include other types of perturbations, such as solar radiation pressure.) In addition, a differential corrections process is employed to ensure position and velocity continuity along the path while satisfying all constraints imposed upon the trajectory. The implementation of this intermediate step is the primary focus of this work. In the final step, the results are numerically integrated using a sun–Earth–moon (SEM) model in which solar and lunar positions are determined from ephemeris data.

This work differs from previous work in the area of multiple-lunar-swingby (MLS) trajectories, such as that of Ishii and Matsuo,[6] by including an intermediate step between the initial approximation and the numerically integrated solution. The application has also been broadened by incorporating initial approximations that may be non-Keplerian. Thus, by incorporating multiconic techniques in the second step, the initial approximation can be improved while the desired orbital characteristics are maintained. Therefore, much of the design work can be accomplished using simpler models, with the knowledge that a viable numerically integrated solution can be obtained.

Background

In the multiple-encounter problem, the primary focus is the identification of a specific solution for the motion of a spacecraft in a restricted three- or four-body problem (R3BP or R4BP). In particular, the methodology is applied in the SEM system. Although it is possible to generalize this approach to other primary systems, the SEM system has been the focus of some recent mission planning, and thus it is the system of choice for this study. To nondimensionalize the problem, then, define the characteristic quantities $G \cdot M^*$, L^*,

Received April 17, 1997; revision received Sept. 12, 1997; accepted for publication Sept. 13, 1997.

*Graduate Student, School of Aeronautics and Astronautics. Member AIAA.

†Professor, School of Aeronautics and Astronautics. E-mail: howell@ecn.purdue.edu. Senior Member AIAA.

and T^* corresponding to the gravitational parameter of the Earth–moon system, the average distance between the Earth and moon, and a characteristic time selected such that $T^* = [L^{*3}/(G \cdot M^*)]^{1/2}$.

The analysis is accomplished using three coordinate systems: Earth inertial (EI), moon inertial (MI), and solar rotating (SR). The first two frames (EI and MI) are the principal working frames used in the problem analysis and are defined as follows. The EI frame $(\hat{X}_e, \hat{Y}_e, \hat{Z}_e)$ has its origin at the center of the Earth and is defined consistent with the mean ecliptic and equinox of 2000. The MI frame $(\hat{X}_m, \hat{Y}_m, \hat{Z}_m)$ has its origin at the center of the moon, and each axis remains parallel to the corresponding axis in the EI frame. The origin of the SR frame $(\hat{x}_s, \hat{y}_s, \hat{z}_s)$ is located at the center of the Earth, with the $\hat{x}_s$ axis parallel to the vector from the sun to the Earth. The $\hat{z}_s$ axis is coincident with the instantaneous angular momentum vector of the Earth about the sun, and thus $\hat{y}_s$ equals $\hat{z}_s \times \hat{x}_s$.

The methodology is heavily based on the use of the state transition matrix (STM). To simplify notation, denote $\Phi_{f,i} = \Phi(t_f, t_i)$ as the STM from time t_i to t_f. The STM can be computed analytically or numerically and is the foundation of the differential corrections procedures used for targeting purposes. A major advantage associated with using the two-body model and conic arcs is the availability of analytic expressions for the elements of the state transition matrix.[7,8] The functional form of these partial derivatives depends on the actual conic reference orbit, either elliptical or hyperbolic. These analytic expressions offer a quick method for the determination of the STM that is extremely useful in the application of the multiconic techniques and can be used in combination with numerical STMs generated with solutions to the R3BP.

Initial Approximation: Conics

To develop a multiple-lunar-swingby trajectory, an initial approximation that satisfies the specified design requirements is sought. As an initial baseline, assume a solution such that all trajectory arcs can be approximated as geocentric two-body conics, thus neglecting the lunar and solar gravity effects. By specifying that each conic segment begin and/or end with a lunar encounter, an approximate MLS trajectory can be created simply by "patching" these geocentric conic segments together at consecutive lunar encounter points. This analysis yields a useful initial approximation to the solution and provides a basis of comparison for the final integrated trajectory.

The motivation for incorporating multiple lunar swingbys into any trajectory may vary, but frequently the goal is to achieve certain orbital characteristics relative to the SR frame. The concept proposed by Farquhar and Dunham,[3] using lunar gravity assists to advance the line of apsides at the rate required to "fix" the orbit in the SR frame, is one such example. The theoretical basis for determining lunar encounters at appropriate time intervals lies in the development of a timing condition relating the motion of the sun, Earth, moon, and spacecraft. The development of this timing condition and the theoretical basis for the initial conic approximation are presented in detail in Refs. 4, 9, and 10. A brief summary of the details is presented here.

Timing Condition

To construct a multiple-lunar-encounter trajectory, a method is required to design a series of Earth-centered conic segments that begin and/or end with lunar encounters and are oriented in the desired direction relative to the SR frame. This approach ensures that the spacecraft and the moon will be in the same vicinity at the appropriate times. From detailed discussions in Refs. 4, 9, and 10, it is apparent that the determination of conic arcs that begin and end in lunar encounters can be reduced to the solution of a single algebraic equation called the timing condition (TC). The functional form of this timing condition, from Howell and Marsh,[9] is an implicit algebraic function of the form

$$\mathrm{TC}(e_m, \chi, \sigma_{0,1,2}, \xi, \eta; a_c, e_c) = 0 \tag{1}$$

The variable e_m represents the eccentricity of the lunar orbit about the Earth with perigee at P_m (Fig. 1). The angle χ, also shown in Fig. 1, describes the orientation of the orbit line of apsides with respect to the lunar line of apsides, measured clockwise from the $\hat{X}$ axis. [Note that the conic reference frame $(\hat{X}, \hat{Y})$ is defined such that $\hat{X}$ is along the line of apsides in the direction of the moon at time $t = 0$, denoted as point R.] The parameters σ_i, ξ, and η are used to uniquely parameterize the Earth-centered orbit, as described in Ref. 9.

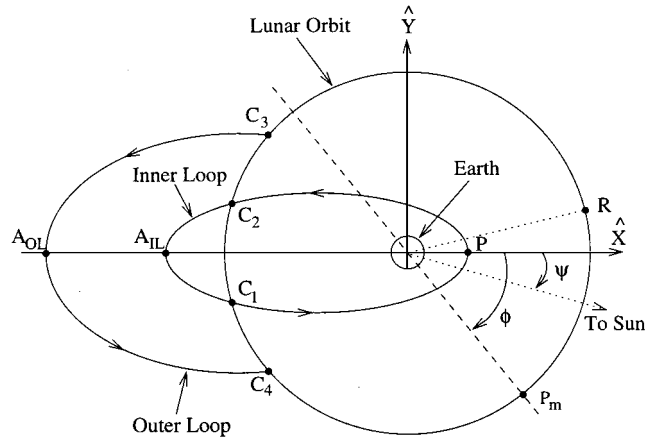

Fig. 1 Conic arc definitions.

The solution of this algebraic function yields two of the orbit parameters, a_c and e_c, associated with the conic segment. In addition, the true anomaly θ_c and the relative time t_c corresponding to the spacecraft location at the endpoints C_i are available. Note that, in the conic reference frame, $t = 0$ is defined at a spacecraft crossing of the line of apsides (at perigee P or apogee A_{OL} or A_{IL}; Fig. 1) according to σ_2. Therefore, due to the near symmetry of the problem, the spacecraft, Earth, and moon will be nearly collinear along the spacecraft line of apsides at $t = 0$.

Conic Arc Selection

Once the conic arc has been determined from the solution of the timing condition, it is necessary to orient this segment in the SR frame with respect to the sun–Earth line ($\hat{x}_s$ axis in the SR frame). It is assumed in the solution process that the conic orbit plane for each segment is coincident with the lunar orbit plane. (This requirement facilitates the conic selection process only and may be relaxed later.) Thus, it is possible to completely define the appropriate conic segment, as well as its orientation, in terms of the lunar orbit. The segment is represented by the orbit parameters a_c, e_c, Ω_{moon}, i_{moon}, θ_c, and t_c at each endpoint (C_i in Fig. 1).

After the conic orbit plane is quantified, orientation of the spacecraft orbit is accomplished through identification of epochs corresponding to appropriate locations of the sun and moon relative to the Earth. Such epochs result from an iterative search through solar and lunar ephemerides. This process is aided by the inherent near symmetry of consecutive collision orbits.[4] The angle ψ (Fig. 1) specifies the orientation of the spacecraft line of apsides with respect to the sun–Earth line. This angle is ideally 0 deg for a trajectory with antisolar pointing apogees and 180 deg for solar pointing apogees.

There are two types of solutions for the conic arcs generated by solution of the timing condition, as shown in Fig. 1. The first type of conic arc is termed an inner loop.[10] For this type, a piece of the conic solution is chosen that contains at least one perigee and some number of apogees during the time from one lunar encounter to the next. The other type of conic segment is called an outer loop[10] and is characterized by conic segments that pass through at least one apogee and some number of perigees between lunar encounters.

For construction of a complete multiple-lunar-encounter path, a series of conic arc segments are patched together at lunar encounters. The arcs must be properly sequenced using the conic arc selection process to ensure an orbit orientation history consistent with the requirements. The entire process of creating a multiple-lunar-encounter trajectory by patching these conic arc segments together is called patched conic analysis (PCA).

This design process requires a set of input parameters that are determined from the design specifications for the mission. These

parameters are used to solve for the orbital elements describing the conic arcs that comprise the initial estimate. The first input is the specification of the injection date for the MLS trajectory in Julian format (JD_1). To facilitate a solution, this date is assumed to correspond to perigee on the first conic segment. The next inputs are the approximate lengths of the conic segments in an integer number of months N_{mos} and the expected number of apogees N_{apos}.

The fourth required input parameter is an estimate of the angle ψ. Because most of the flight time is spent in the outer loops, it is desirable for these segments to match this specification as closely as possible. For inner loops, however, it is often desirable from a mission design standpoint to specify the perigee passage distance R_p in addition to ψ. This specification usually results in some loss of control over the orientation angle ψ for the segment, but because the inner loops are generally shorter in duration than the outer loops, this loss is not crucial to overall trajectory planning.

Given these inputs (JD_1, N_{mos}, N_{apos}, ψ, and possibly R_p) that reflect the desirable characteristics for each Earth-centered conic, the conic arc selection algorithm solves the TC iteratively, as described in Ref. 10, for the properly oriented conic arc segments that best match the mission specifications. From the solution of the TC, the orbit parameters representing the conic arcs and the dates of the lunar encounters are obtained. All conic segments are then patched together at lunar encounter points to create the two-body approximation to the solution of the MLS problem.

Initial Approximation: Restricted Three-Body Problem

Another approach for construction of an initial approximation involves solutions to a restricted three-body problem. One example is a transfer from the Earth to a sun–Earth libration-point orbit using one or more lunar gravity assists. In this case, the final state for the MLS trajectory is chosen to coincide with a time and position state along a stable manifold associated with a predetermined libration-point orbit (LPO).[5] This manifold state is then targeted by the trajectory arc selection algorithm to create a transfer from the Earth to the vicinity of the LPO. A deterministic injection $\Delta \boldsymbol{V}$ at the final state completes the transfer to the libration-point orbit.

Targeting of the final state on the MLS trajectory is accomplished using two different methods, depending on the desired solution. In the first method, the conic arcs leading to the final lunar encounter are determined, and a two-body Lambert solution is generated between the final lunar encounter and the desired final position state. This method is used to obtain the initial approximation of the transfer that includes one or more lunar gravity assists. In the second method, a portion of the manifold (propagated backward from the LPO to the Earth) is employed as the approximation of the final segment in the trajectory. This type of initial approximation is especially relevant for those MLS solutions with one lunar encounter or no lunar encounters.

Results from Patched Conic Analysis

The first example of a multiple-lunar-swingby trajectory is composed of four conic segments: two inner loops and two outer loops. For this trajectory, it is specified that the spacecraft apogees switch from an orientation in the antisolar ($+\hat{\boldsymbol{x}}_s$) direction to the solar ($-\hat{\boldsymbol{x}}_s$) direction, creating a "butterfly" trajectory. An injection date of JD 2450573.0 is specified for the first segment, corresponding to a conic orbit perigee on April 4, 1997. The input parameters associated with the conic segments that result from the patched conic algorithm are shown in Table 1. The conic arc elements a_c and e_c from the solution of the TC, as well as the actual trajectory duration, are also shown for each of the four segments in the trajectory.

The second example of an MLS trajectory is a transfer to the vicinity of the sun–Earth L_2 libration point using a single lunar flyby. For this case, an initial date of JD 2451547.3 is specified for the injection segment, corresponding to a conic orbit perigee on Nov. 4, 1999. The end state is selected to coincide with a specified Lissajous orbit and its associated stable manifold.[5] The following is representative of a state on the manifold: $x_s = 1{,}262{,}748$ km, $y_s = -204{,}731$ km, and $z_s = -43{,}300$ km relative to the SR frame on JD 2451593.6. To generate a transfer path from the Earth to the target point, a variety of approaches might be used to produce an initial

Table 1 Input/output parameters for butterfly example

Parameter	Segment 1	2	3	4
		Inputs		
N_{mos}	1	2	6	2
N_{apos}	1	1	3	1
R_p, km	6,578	——	80,000	——
ψ, deg	0.0	0.0	90.0	180.0
		Outputs		
a_c / L^*	0.56059	1.86946	1.50160	1.87954
e_c	0.96947	0.81973	0.86140	0.80178
Δt, days	15.4276	63.7251	157.4934	64.2000

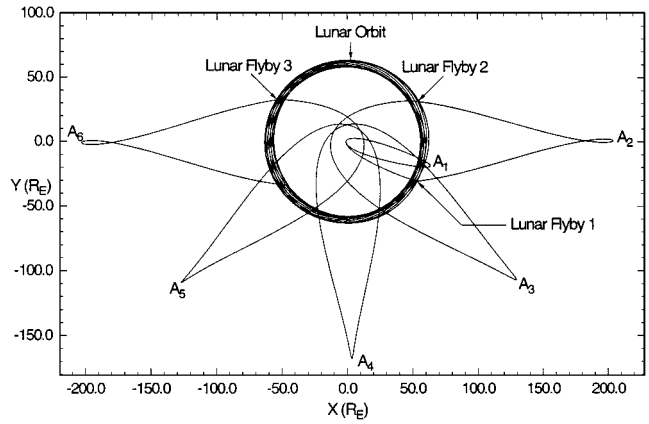

Fig. 2 Butterfly example: PCA.

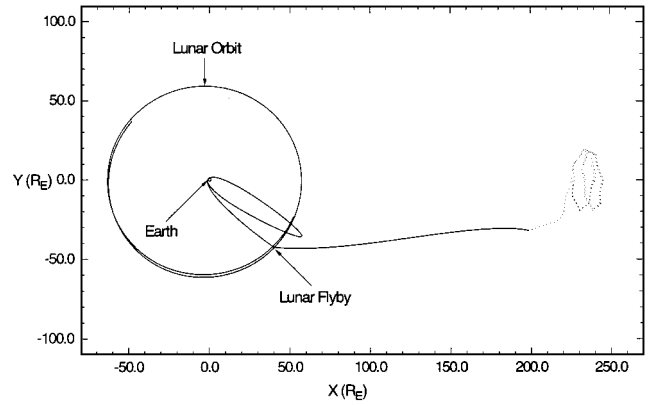

Fig. 3 Earth-to-L_2 transfer example: PCA.

approximation. In this case, an initial conic arc associated with the phasing loops is determined with a nondimensional $a_c = 0.56946$ and an eccentricity $e_c = 0.96995$, similar to the first example. Then, given the position and date of the lunar encounter, the final trajectory segment is initially approximated as a conic that connects the lunar encounter with the target position and date from a numerical solution of the R4BP.

The resulting trajectories are projected onto the $\hat{\boldsymbol{x}}_s$–$\hat{\boldsymbol{y}}_s$ plane in the SR frame and shown in Figs. 2 and 3. The four-arc butterfly solution is shown in Fig. 2 and clearly meets the desired change in solar orientation angle. The LPO transfer example is shown in Fig. 3, where the dashed line denotes the continuation of the manifold and the desired Lissajous orbit (as a numerically computed solution of the R4BP). From the view of the trajectory in the SR frame, it is evident that this process of patching together two- and four-body arcs yields a reasonable approximation to solutions of the MLS problem that meet the design requirements. However, by neglecting the lunar and solar gravity in the conic arcs, errors are introduced into the solution. These errors are evidenced as large equivalent velocity discontinuities at the lunar collision points and (not surprisingly) a significant velocity discontinuity at the patch point between the two- and four-body arcs. The poor modeling of the lunar encounters

in PCA generally prevents the straightforward extension of the solution to produce a numerically integrated trajectory with the same design characteristics. Therefore, it becomes necessary to improve the initial results so that a viable trajectory can be constructed.

Multiconic Analysis

As an intermediate step between the initial approximation and numerical integration in the four-body problem, a three-body model with solar perturbations is employed to enable any initial result to serve as the basis for an improved solution of the MLS problem. The goal in this step is to employ the approximation techniques in a manner that will ultimately lead to a numerically integrated trajectory that retains the overall orbit characteristics designed in the preliminary step.

The differential equations governing motion in the restricted three-body problem are not, in general, solvable analytically. However, a number of authors have developed approximations that provide a reasonable representation of the spacecraft motion under various conditions. The solution approach used here is based on those developed by Wilson[11] and Byrnes and Hooper,[12] among others, and is called multiconics.

When using multiconics, the contributions of each primary to the motion of the spacecraft are evaluated separately as solutions to a two-body problem and then "overlapped" through the addition of a constant velocity segment. The result is an approximation to motion in the restricted three-body problem or the restricted four-body problem if solar perturbations are included. Because a solution generated with multiconics includes the gravitational effects of additional primaries, it should provide a more accurate method of representing the motion in the MLS problem or the Earth-to-L_i transfer problem.

State Transition Matrices Using Multiconics

Although, in general, no analytic solution is available for the STM in the R3BP or R4BP, the use of two-body conics in the multiconic approximations allows analytic representations for the elements of the STM to be developed from the appropriate two-body STMs.[7,8] The STM for a single multiconic step may be determined by sequentially multiplying the STMs corresponding to each propagation step in the algorithm.

As an example, consider a spacecraft moving from the Earth to the moon. The first step yields an STM from propagation of the Earth-centered conic, using the appropriate two-body solution. This matrix relates the initial geocentric state to the final state of the Earth-centered conic (EC) and is denoted $\Phi^{\mathrm{EC}}_{f,i}$. Next, the final geocentric state is transformed to a selenocentric state, and the effects due to primary motion and solar perturbations are added. The transformation and effects of the primary motion do not affect the STM; however, the addition of solar perturbations does contribute by changing the end state on the EC conic in some specified manner. The effective STM for this segment is denoted $\Phi^{\mathrm{sun}}_{f,f}$. In the field-free segment (motion under no gravitational force fields), the state is propagated backward along the selenocentric velocity vector to the initial time. The STM corresponding to the field-free trajectory, $\Phi^{\mathrm{FF}}_{i,f}$, is simply a linear function of the propagation time. In the final step of the algorithm, a moon-centered conic (MC) is propagated forward in time to obtain the approximation to the final selenocentric state. This conic STM is denoted $\Phi^{\mathrm{MC}}_{f,i}$ and relates the initial state on the MC to the final selenocentric state. Because all of the STMs are defined relative to the inertial frame, the determination of the complete STM that maps changes in the initial state of the multiconic step to changes in the final state involves multiplying these four matrices sequentially to obtain

$$\Phi^{\mathrm{step}}_{f,i} = \Phi^{\mathrm{MC}}_{f,i}\Phi^{\mathrm{FF}}_{i,f}\Phi^{\mathrm{sun}}_{f,f}\Phi^{\mathrm{EC}}_{f,i} \tag{2}$$

A similar STM can be computed for each of the multiconic steps along a given path. These matrices then can be sequentially multiplied to create the STM for the entire trajectory segment. This matrix associated with the multiconic approximation of the trajectory segment is employed in various differential corrections procedures to target desired end states for the MLS/LPO problem.

Pseudostate Theory

Application of the multiconic technique, as described earlier, is very successful at approximating specific state vectors in the R3BP or R4BP. However, the algorithm becomes less effective if the trajectory includes a close passage of the second primary (in this case, the moon). Because modeling of the lunar flybys is one of the primary reasons for using multiconics in the analysis, a modified version of the multiconic algorithm must be employed. This modified algorithm, based on the original development by Wilson[11] in conjunction with the algorithm of Byrnes and Hooper,[12] is based on pseudostate theory. The basic approximations are the same as those associated with the preceding multiconic algorithm, but it effectively models hyperbolic trajectories relative to the moon.

A state transition matrix can also be computed for the pseudostate approximation by sequentially multiplying the STM for each of the propagation steps. This pseudostate STM is crucial in the determination of the lunar swingby through the solution of a three-body Lambert problem (3BLP). Among various attempts at approximating the solution of the 3BLP, a particularly appropriate solution approach was proposed by Byrnes[13] using pseudostate theory and the resulting STM in a differential corrections process. This procedure, modified to include solar gravity, forms the basis of the targeting scheme to identify a solution that passes through specified position states before and after the lunar flyby or, in other words, to bridge the "gaps" in the solution left by the poor modeling of the lunar encounter using PCA. These specified states (termed swingby states) around the lunar flybys are determined from the initial approximation and represent the boundary between the two types of multiconic algorithms. The swingby states are determined by terminating the trajectory arcs surrounding the lunar encounters at a predetermined lunar sphere of influence. A value of 25 Earth radii has been found to yield a reasonable balance between accuracy and multiconic efficiency.

Algorithm

To apply the multiconic approximations to the given problem, it is necessary that a discrete set of states (termed patch points) be available to start the algorithm. From the initial approximation, state vectors representing the initial and final states, the swingby states corresponding to each lunar encounter, and other desired states, such as apogee locations, are available for each of the segments.

Between the endpoints of all nonswingby segments, basic multiconic theory is applied to generate an updated solution for that segment. To begin, the total flight time for the segment under consideration is subdivided to obtain a multiconic step size Δt of roughly 6 h. It has been determined that a multiconic step of this size yields sufficient accuracy in the sun–Earth–moon problem without sacrificing computational speed. The first multiconic step is propagated from the initial time t_i to the time $t_j = t_i + \Delta t$, and the state transition matrix $\Phi^{\mathrm{step}}_{j,i}$ for this step is computed using two-body approximations. The end state at the final time t_j then becomes the initial state for the next step, and the process is repeated until the final time for the entire trajectory segment is reached.

The position state at the end of the final multiconic step is compared with the desired final state for the segment. If the difference between the position states is greater than a specified tolerance, the complete STM for the segment is used to differentially correct the velocity state at the initial point on the segment to eliminate the error. Note that, in this differential corrections process, the initial position state and time remain unchanged. This entire process is repeated until the final position state is within the prescribed tolerance. This algorithm, hereafter denoted multiconic analysis (MCA), is repeated for each of the nonswingby segments along the MLS trajectory.

After MCA is applied to the nonswingby segments and the states at the patch points are updated, it is necessary to model the lunar flybys to create a trajectory that is continuous in position and time. Pseudostate analysis (PSA) is used between the swingby states of the encounter segments to model the lunar flybys.

For use as input to PSA, the updated states of the patch points are available from the MCA segment solutions. Between the initial and final swingby states of a given encounter segment, a two-body

Lambert problem (relative to the moon) is solved to yield an estimate of the lunar periapsis state and the time of closest approach. After the initial estimate of the perilune state is computed, the lunar swingby is approximated by application of the Byrnes pseudostate procedure[13] to produce a trajectory arc between the initial and final swingby states. This procedure yields a more accurate estimate of the perilune state, as well as a second estimate of the velocity states at the swingby points.

At this stage, the trajectory has position and time continuity. However, effective velocity discontinuities may now be present at each patch point (excluding the initial and final states). The current estimate of the outgoing velocity state $\boldsymbol{V}_n^+$ at any patch point n is compared with the incoming velocity state $\boldsymbol{V}_n^-$ to compute the patch point velocity discontinuities, that is,

$$\Delta \boldsymbol{V}_n = \boldsymbol{V}_n^+ - \boldsymbol{V}_n^- \tag{3}$$

These patch point $\Delta \boldsymbol{V}$ are computed in EI coordinates. The reduction of these velocity discontinuities is the next step.

Reduction of Velocity Discontinuities

The ultimate goal in the second step of the solution process is a multiple-lunar-swingby trajectory that meets the design specifications and is continuous in both position and time, as well as velocity. In addition, any constraints placed on the trajectory, such as launch conditions or trajectory end-state requirements, must be satisfied. Thus, it is desired to create an automated process to simultaneously reduce the patch point velocity discontinuities throughout the solution while incorporating any constraints. This process is accomplished by varying the patch point state positions and times in a specified manner using a differential corrections scheme. The resulting various patch point $\Delta \boldsymbol{V}$ can be reduced significantly, if not eliminated altogether, while the desired characteristics of the solution are retained so that the numerically integrated trajectory accurately reflects the design specifications.

The cost associated with the multiconic estimate is defined as the sum of the magnitudes of all of the velocity discontinuities along the trajectory (ΔV_{tot}) plus any constraint penalties. This cost must be minimized while retaining the trajectory characteristics designed in the initial approximation. Define, then, a velocity discontinuity vector $\Delta \boldsymbol{V}_i$ in EI coordinates at each of the patch points consistent with Eq. (3). The subscript i denotes the patch point number ordered sequentially along the trajectory beginning with the initial state. (Note that no effective velocity discontinuities exist at the initial and final states along the trajectory.) The patch point states themselves are also expressed using the i subscript convention.

Derivation of the State Relationship Matrix

To employ a differential corrections process to reduce the total cost, it is necessary to derive the relationships between a given patch point $\Delta \boldsymbol{V}_i$ or constraint α_k and the independent variables in the problem. Because the multiple-lunar-swingby trajectory is described in terms of discrete patch point positions and times, it is appropriate to choose these quantities as the independent parameters. Therefore, it is necessary to determine the variation of each $\Delta \boldsymbol{V}_i$ and each constraint α_k due to variations in the patch point positions and times, which have thus far been fixed at values determined during the initial approximation. A linear relationship between these states can be represented in matrix form as

$$\begin{Bmatrix} \delta \Delta \boldsymbol{V}_i \\ \delta \alpha_k \end{Bmatrix} = M \begin{Bmatrix} \delta \boldsymbol{R}_j \\ \delta t_j \end{Bmatrix} \tag{4}$$

where

$$M = \begin{bmatrix} \dfrac{\partial \Delta \boldsymbol{V}_i}{\partial \boldsymbol{R}_j} & \dfrac{\partial \Delta \boldsymbol{V}_i}{\partial t_j} \\ \dfrac{\partial \alpha_k}{\partial \boldsymbol{R}_j} & \dfrac{\partial \alpha_k}{\partial t_j} \end{bmatrix} \tag{5}$$

and $\boldsymbol{R}_j$ and t_j denote the position and time corresponding to the jth patch point state. Notice that the matrix M (called the state relationship matrix or SRM) is not square; that is, there are more independent variables ($\boldsymbol{R}_j$ and t_j) than there are dependent variables ($\Delta \boldsymbol{V}_i$ and α_k). Because this system is underdetermined, there are infinitely many solutions, and it is therefore possible to estimate the changes in the values of the independent variables that are necessary to reduce $\Delta \boldsymbol{V}_i$, α_k, and, thus, the total cost. Note that if, through the addition of constraints, the system becomes overdetermined, it is still possible to add flexibility and maintain the underdetermined nature by including additional patch points in the analysis. Although the size of the SRM can be large, this disadvantage is offset by the fact that the STMs from MCA/PSA can be used to produce expressions for each partial derivative in the matrix.[1,2]

Variations of ΔV_i with Positions

To determine analytic expressions for the elements in the SRM, begin by examining the general relationship between any velocity discontinuity $\Delta \boldsymbol{V}_n$ and changes in the independent position states. Split $\Delta \boldsymbol{V}_n$ into its component parts, as in Eq. (3), and consider each partial derivative with respect to a position state vector $\boldsymbol{R}_j$. The corresponding elements in the SRM become

$$\frac{\partial \Delta \boldsymbol{V}_n}{\partial \boldsymbol{R}_j} = \frac{\partial \boldsymbol{V}_n^+}{\partial \boldsymbol{R}_j} - \frac{\partial \boldsymbol{V}_n^-}{\partial \boldsymbol{R}_j} \tag{6}$$

Because the trajectory segments between consecutive patch points with a given time of flight are solutions of a four-body Lambert problem (4BLP), the Lambert partials discussed in Ref. 14 can be used to evaluate the partials in Eq. (6). The elements of the state transition matrices that appear in these Lambert partials are already available from MCA/PSA. From the three patch point position states that surround the velocity discontinuity ($\boldsymbol{R}_{n-1}$, $\boldsymbol{R}_n$, and $\boldsymbol{R}_{n+1}$), two trajectory arcs from $n-1$ to n and from n to $n+1$ can be identified. The corresponding STMs, $\Phi_{n,n-1}$ and $\Phi_{n+1,n}$, can be written in terms of four 3×3 submatrices, for example,

$$\Phi_{n,n-1} = \begin{bmatrix} \dfrac{\partial \boldsymbol{R}_n}{\partial \boldsymbol{R}_{n-1}} & \dfrac{\partial \boldsymbol{R}_n}{\partial \boldsymbol{V}_{n-1}^+} \\ \dfrac{\partial \boldsymbol{V}_n^-}{\partial \boldsymbol{R}_{n-1}} & \dfrac{\partial \boldsymbol{V}_n^-}{\partial \boldsymbol{V}_{n-1}^+} \end{bmatrix} = \begin{bmatrix} A_{n,n-1} & B_{n,n-1} \\ C_{n,n-1} & D_{n,n-1} \end{bmatrix} \tag{7}$$

From Ref. 2, the nonzero variations of $\Delta \boldsymbol{V}_n$ with the positions $\boldsymbol{R}_j$ are

$$\frac{\partial \Delta \boldsymbol{V}_n}{\partial \boldsymbol{R}_{n-1}} = -B_{n-1,n}^{-1} \tag{8}$$

$$\frac{\partial \Delta \boldsymbol{V}_n}{\partial \boldsymbol{R}_n} = -B_{n+1,n}^{-1} A_{n+1,n} + B_{n-1,n}^{-1} A_{n-1,n} \tag{9}$$

$$\frac{\partial \Delta \boldsymbol{V}_n}{\partial \boldsymbol{R}_{n+1}} = B_{n+1,n}^{-1} \tag{10}$$

The partials of $\Delta \boldsymbol{V}_n$ with respect to all other patch point positions can be shown to be zero because the velocities at any given patch point are related only to the 4BLP solutions directly preceding and following it. The expressions in Eqs. (8–10) can be readily evaluated from the STMs determined during MCA/PSA. The results are used to form the partials that appear in the M matrix in Eq. (4), that is, the partials relating $\Delta \boldsymbol{V}_i$ to changes in the patch point position states.

Variations of ΔV_i with Times

It is also necessary to determine the partial derivatives of $\Delta \boldsymbol{V}_i$ with respect to the times associated with each patch point state. The process is similar to the one used to determine the partials with respect to the patch point positions. Now, however, it is necessary to include the effect of a differential change in time in the expression for the state differentials.

First, note that the change in state due to a differential change in time, δt, can be estimated by a first-order approximation as

$$\delta \boldsymbol{R}(t + \delta t) = \delta \boldsymbol{R}(t) + \boldsymbol{V} \delta t \tag{11}$$

$$\delta \boldsymbol{V}(t + \delta t) = \delta \boldsymbol{V}(t) + \boldsymbol{a}(t) \delta t \tag{12}$$

where $\boldsymbol{a}$ is the inertial acceleration of the spacecraft at the given instant t.

Return again to the matrix M and write the expression relating the change in $\Delta \boldsymbol{V}_n$ to the change in time t_j as follows:

$$\frac{\partial \Delta \boldsymbol{V}_n}{\partial t_j} = \frac{\partial \boldsymbol{V}_n^+}{\partial t_j} - \frac{\partial \boldsymbol{V}_n^-}{\partial t_j} \tag{13}$$

Consistent with the procedure for the position differentials, the nonzero variations of $\Delta \boldsymbol{V}_n$ with respect to the times t_j are evaluated as[2]

$$\frac{\partial \Delta \boldsymbol{V}_n}{\partial t_{n-1}} = B_{n-1,n}^{-1} \boldsymbol{V}_{n-1}^+ \tag{14}$$

$$\frac{\partial \Delta \boldsymbol{V}_n}{\partial t_n} = B_{n+1,n}^{-1} A_{n+1,n} \boldsymbol{V}_n^+ - B_{n-1,n}^{-1} A_{n-1,n} \boldsymbol{V}_n^- \tag{15}$$

$$\frac{\partial \Delta \boldsymbol{V}_n}{\partial t_{n+1}} = -B_{n+1,n}^{-1} \boldsymbol{V}_{n+1}^- \tag{16}$$

The partials of $\Delta \boldsymbol{V}_n$ with respect to the other patch point times are zero. The expressions in Eqs. (14–16) are evaluated using the STMs computed in MCA/PSA and from the velocity states at the patch points. These elements are appropriately placed in the M matrix in Eq. (4) to complete the upper half of the SRM.

Constraint Variations

To incorporate any constraints into the solution process, it is necessary to determine the variations of those constraints with respect to variations in the independent parameters. The constraints that are examined in this study can be placed into one of two categories: launch constraints or end-state targeting constraints.

For launch, four conditions are of greatest concern, namely, launch altitude, launch date, launch inclination, and insertion as close to perigee as possible. Examine each, beginning with launch altitude. Because altitude is related to the independent parameters through the magnitude of the initial position $\boldsymbol{R}_1$, the constraint can be written as

$$\alpha_1 = |\boldsymbol{R}_1| - R_{\text{des}} \tag{17}$$

where R_{des} is the desired launch altitude. Thus, the variation is expressed as

$$\frac{\partial \alpha_1}{\partial \boldsymbol{R}_1} = \frac{\boldsymbol{R}_1^T}{|\boldsymbol{R}_1|} \tag{18}$$

Similarly, because launch date is actually the independent parameter t_1, the functional form of the constraint is

$$\alpha_2 = t_1 - t_{\text{des}} \tag{19}$$

where t_{des} is the desired launch date. The variation is then

$$\frac{\partial \alpha_2}{\partial t_1} = 1 \tag{20}$$

From the definition of the inclination i in terms of the pole vector of the Earth $\hat{Z}_{\text{eq}}$,

$$\cos i = \frac{\boldsymbol{R}_1 \times \boldsymbol{V}_1}{|\boldsymbol{R}_1 \times \boldsymbol{V}_1|} \cdot \hat{Z}_{\text{eq}} \tag{21}$$

where $\cdot$ denotes the dot product. The functional form for the inclination constraint is expressed as

$$\alpha_3 = \cos i - \cos i_{\text{des}} \tag{22}$$

where i_{des} is the desired inclination relative to the Earth equator and equinox of the launch date. Consequently, the total variation can be written as

$$d\alpha_3 = \frac{\partial \alpha_3}{\partial \boldsymbol{R}_1} \delta \boldsymbol{R}_1 + \frac{\partial \alpha_3}{\partial \boldsymbol{V}_1} \delta \boldsymbol{V}_1 \tag{23}$$

Now using Eq. (18) and the trigonometric identities

$$(\boldsymbol{R}_1 \times \boldsymbol{V}_1) \cdot \hat{Z}_{\text{eq}} = (\hat{Z}_{\text{eq}} \times \boldsymbol{R}_1) \cdot \boldsymbol{V}_1 = (\boldsymbol{V}_1 \times \hat{Z}_{\text{eq}}) \cdot \boldsymbol{R}_1 \tag{24}$$

and

$$|\boldsymbol{R}_1 \times \boldsymbol{V}_1| = \left[|\boldsymbol{R}_1|^2 |\boldsymbol{V}_1|^2 - (\boldsymbol{R} \cdot \boldsymbol{V}_1)^2 \right]^{\frac{1}{2}} \tag{25}$$

it follows that

$$\frac{\partial \cos i}{\partial \boldsymbol{R}_1} = \frac{(\boldsymbol{V}_1 \times \hat{Z}_{\text{eq}})^T}{|\boldsymbol{R}_1 \times \boldsymbol{V}_1|} - \cos i \cdot \frac{|\boldsymbol{V}_1|^2 \boldsymbol{R}_1^T - (\boldsymbol{R}_1 \cdot \boldsymbol{V}_1) \boldsymbol{V}_1^T}{|\boldsymbol{R}_1 \times \boldsymbol{V}_1|^2} \tag{26}$$

and

$$\frac{\partial \cos i}{\partial \boldsymbol{V}_1} = \frac{(\hat{Z}_{\text{eq}} \times \boldsymbol{R}_1)^T}{|\boldsymbol{R}_1 \times \boldsymbol{V}_1|} - \cos i \cdot \frac{|\boldsymbol{R}_1|^2 \boldsymbol{V}_1^T - (\boldsymbol{R}_1 \cdot \boldsymbol{V}_1) \boldsymbol{R}_1^T}{|\boldsymbol{R}_1 \times \boldsymbol{V}_1|^2} \tag{27}$$

Return to Eq. (23) and note that $\delta \boldsymbol{R}_1$ is one of the independent variables in the problem but $\delta \boldsymbol{V}_1$ depends on the positions and times according to the relationship

$$\delta \boldsymbol{V}_1 = \frac{\partial \boldsymbol{V}_1}{\partial \boldsymbol{R}_1} \delta \boldsymbol{R}_1 + \frac{\partial \boldsymbol{V}_1}{\partial t_1} \delta t_1 + \frac{\partial \boldsymbol{V}_1}{\partial \boldsymbol{R}_2} \delta \boldsymbol{R}_2 + \frac{\partial \boldsymbol{V}_1}{\partial t_2} \delta t_2 \tag{28}$$

Each of the partials in Eq. (28) is a Lambert partial, as described in the preceding sections,[14] so that from Eq. (23) the variations are expressed as

$$\frac{\partial \alpha_3}{\partial \boldsymbol{R}_1} = \frac{\partial \cos i}{\partial \boldsymbol{R}_1} - \frac{\partial \cos i}{\partial \boldsymbol{V}_1} \cdot B_{2,1}^{-1} A_{2,1} \tag{29}$$

$$\frac{\partial \alpha_3}{\partial t_1} = \frac{\partial \cos i}{\partial \boldsymbol{V}_1} \cdot \left(\boldsymbol{a}_1 + B_{2,1}^{-1} A_{2,1} \boldsymbol{V}_1 \right) \tag{30}$$

$$\frac{\partial \alpha_3}{\partial \boldsymbol{R}_2} = \frac{\partial \cos i}{\partial \boldsymbol{V}_1} \cdot B_{2,1}^{-1} \tag{31}$$

$$\frac{\partial \alpha_3}{\partial t_2} = -\frac{\partial \cos i}{\partial \boldsymbol{V}_1} \cdot B_{2,1}^{-1} \boldsymbol{V}_2 \tag{32}$$

Finally, the function for the apse launch constraint, $\boldsymbol{R}_1 \cdot \boldsymbol{V}_1 = 0$, is defined to be

$$\alpha_4 = \boldsymbol{R}_1 \cdot \boldsymbol{V}_1 \tag{33}$$

The partials due to position and velocity are simply

$$\frac{\partial (\boldsymbol{R}_1 \cdot \boldsymbol{V}_1)}{\partial \boldsymbol{R}_1} = \boldsymbol{V}_1^T \tag{34}$$

$$\frac{\partial (\boldsymbol{R}_1 \cdot \boldsymbol{V}_1)}{\partial \boldsymbol{V}_1} = \boldsymbol{R}_1^T \tag{35}$$

Thus, the variations of α_4 with respect to the independent variables can be written as

$$\frac{\partial \alpha_4}{\partial \boldsymbol{R}_1} = \boldsymbol{V}_1^T - \boldsymbol{R}_1^T \cdot B_{2,1}^{-1} A_{2,1} \tag{36}$$

$$\frac{\partial \alpha_4}{\partial t_1} = \boldsymbol{R}_1^T \cdot \left(\boldsymbol{a}_1 + B_{2,1}^{-1} A_{2,1} \boldsymbol{V}_1 \right) \tag{37}$$

$$\frac{\partial \alpha_4}{\partial \boldsymbol{R}_2} = \boldsymbol{R}_1^T \cdot B_{2,1}^{-1} \tag{38}$$

$$\frac{\partial \alpha_4}{\partial t_2} = -\boldsymbol{R}_1^T \cdot B_{2,1}^{-1} \boldsymbol{V}_2 \tag{39}$$

A second type of constraint is the end-state $(\boldsymbol{R}_N, t_N, \boldsymbol{V}_N)$ constraint. This constraint is used to target a desired final state $(\boldsymbol{R}_{\text{des}}, t_{\text{des}}, \boldsymbol{V}_{\text{des}})$ for the complete trajectory. The constraint functions are formally stated as

$$\alpha_{(5-7)} = \boldsymbol{R}_N - \boldsymbol{R}_{\text{des}} \tag{40}$$

$$\alpha_8 = t_N - t_{\text{des}} \tag{41}$$

$$\alpha_{(9-11)} = \boldsymbol{V}_N - \boldsymbol{V}_{\text{des}} \tag{42}$$

and the related variations with respect to the independent variables are

$$\frac{\partial \alpha_{(5-7)}}{\partial \boldsymbol{R}_N} = I \tag{43}$$

$$\frac{\partial \alpha_8}{\partial t_N} = 1 \tag{44}$$

$$\frac{\partial \alpha_{(9-11)}}{\partial \boldsymbol{R}_N} = -B^{-1}_{N-1,N}\, A_{N-1,N} \tag{45}$$

$$\frac{\partial \alpha_{(9-11)}}{\partial t_N} = \boldsymbol{a}_N + B^{-1}_{N-1,N} A_{N-1,N} \boldsymbol{V}_N \tag{46}$$

$$\frac{\partial \alpha_{(9-11)}}{\partial \boldsymbol{R}_{N-1}} = B^{-1}_{N-1,N} \tag{47}$$

$$\frac{\partial \alpha_{(9-11)}}{\partial t_{N-1}} = -B^{-1}_{N-1,N} \boldsymbol{V}_{N-1} \tag{48}$$

where I is the 3×3 identity matrix. By appropriate choice of the independent parameters, any constraint functions active in the solution can be driven to zero, thus enforcing the constraints.

Reduction Algorithm

The $\Delta \boldsymbol{V}_i$ reduction and constraint enforcement procedure begins with the discrete set of patch point states and times. For each nonswingby segment, MCA is applied between the initial and final patch point states. The updated patch point states are then employed by PSA to generate a second estimate of the velocity states at the swingby points surrounding the flybys. The patch point $\Delta \boldsymbol{V}_i$ and constraint penalties are computed, and the total cost is checked against a desired tolerance. The SRM in Eq. (4) is used in a differential corrections process to compute changes in the independent variables (positions and times) in an attempt to reduce all of the velocity discontinuities in the trajectory and to satisfy any constraints simultaneously.

As noted, the system is underdetermined, and the SRM in Eq. (4) is not invertible. Out of all possible changes in positions and times, choose the one with the smallest Euclidean norm, that is,

$$\begin{Bmatrix} \delta \boldsymbol{R}_j \\ \delta t_j \end{Bmatrix} = M^T (M M^T)^{-1} \begin{Bmatrix} \delta \Delta \boldsymbol{V}_i \\ \delta \alpha_k \end{Bmatrix} \tag{49}$$

where the differential changes in $\Delta \boldsymbol{V}_i$ and α_k are chosen to reduce the total cost. The differential changes for positions and times computed in Eq. (49) are added to the patch point states, which are then used to recompute an estimate of the trajectory with a cost that is lower than that of the preceding solution. This process is repeated until the cost is minimized to within some tolerance. Note that, although Eq. (49) is a linear estimate of the changes, multiple iterations are required due to the nonlinear nature of the motion.

The final trajectory approximated from MCA/PSA is continuous in velocity and satisfies all constraints. These results are then input to a numerical propagation routine to achieve the final desired trajectory. In practice, it was determined that the jump from PCA to MCA/PSA, including the solar perturbations, was often too great for the differential corrections process. In this case, MCA is applied to the PCA results using only the lunar gravity. After an acceptable convergence has been achieved, the solar perturbations are added[12] and the four-body approximation is obtained.

Results

The improved trajectory from MCA/PSA is viewed in the SR frame as a projection onto the $\hat{\boldsymbol{x}}_s$–$\hat{\boldsymbol{y}}_s$ plane (Figs. 4 and 5). The trajectories include all of the propagation steps that comprise the MCA and PSA procedures. The "spikes" represent the various propagation steps and are not representative of the "true" path. Although the MCA/PSA solution actually consists of a set of discrete solution states, plotting all of the various steps in the MCA/PSA algorithms shows the general characteristics of the trajectory quite well.

The results for the butterfly trajectory include the following launch constraints: altitude = 200 km, inclination = 28.5 deg, and

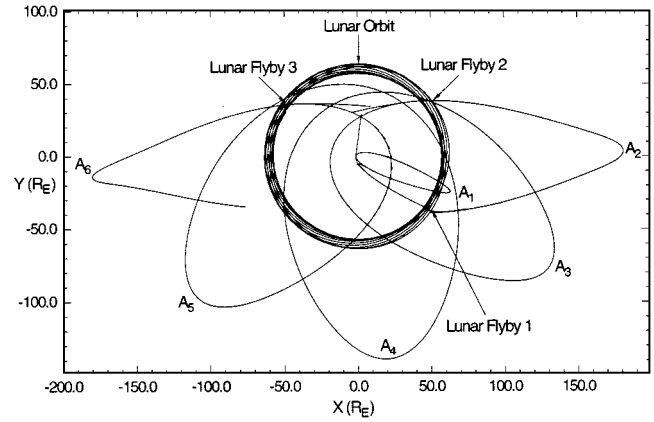

Fig. 4 Butterfly example: constrained.

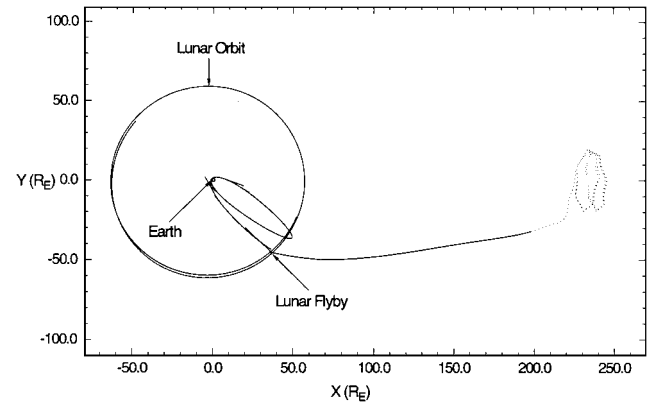

Fig. 5 Earth-to-L_2 transfer example: constrained.

trajectory insertion at perigee. The Earth-to-L_2 transfer mission has similar launch constraints and, in addition, constraints are placed on the end-state position and date, specifying the values to be those obtained from the initial analysis. As mentioned, the end state is numerically generated in the R4BP using manifold theory[5] to determine transfer characteristics for injection onto a path that asymptotically approaches a Lissajous orbit about the sun–Earth L_2 libration point. In the MCA/PSA solution obtained here, the velocity at the end state was not constrained, and so a relatively small velocity discontinuity exists in patching these results to the Lissajous. However, experience suggests that the Lissajous insertion $\Delta \boldsymbol{V}$ can be reduced by moving the end state along the manifold. These results demonstrate this technique's utility in designing MLS and LPO transfer trajectories with constraints.

Final Results

As a final step, it is necessary to demonstrate that the resulting multiconic approximation has produced position and velocity states that can be successfully integrated to generate a viable estimate of the complete trajectory. The model for numerical integration includes the relative four-body equations of motion for the sun–Earth–moon system using the Jet Propulsion Laboratory 202 ephemerides. The numerical accuracy of the results is on the order of 10^{-12} nondimensional units. It is demonstrated in Ref. 2 that, once the converged solution has been obtained from MCA/PSA, the numerical integration proceeds without any degradation of the solution.

The results appear graphically in Figs. 6 and 7 as projections in the $\hat{\boldsymbol{x}}_s$–$\hat{\boldsymbol{y}}_s$ plane. Comparisons can easily be made to the corresponding trajectory approximations from PCA (Figs. 2 and 3) and from MCA/PSA after the SRM reduction process (Figs. 4 and 5). No significant numerical differences between the integrated results and the previous MCA/PSA solutions appear in either case.

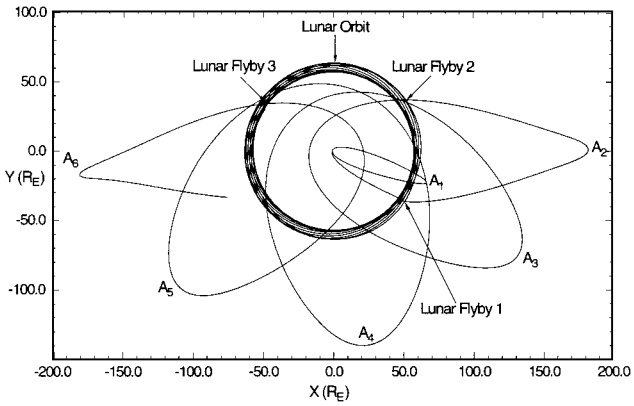

Fig. 6 Butterfly example: integrated.

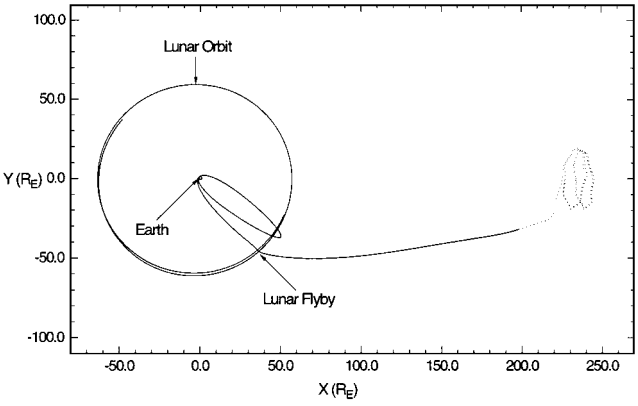

Fig. 7 Earth-to-L_2 transfer: integrated.

Conclusions

In summary, using patched conic analysis and the solution of the timing condition, it is possible to generate multiple-lunar-swingby or libration-point orbit transfer trajectories that meet the given design requirements. However, patched conic analysis introduces errors into the solution due to its failure to adequately model and incorporate the solar and lunar gravity. Using multiconic/pseudostate analysis, it is possible to improve upon the initial solution while maintaining the desired design characteristics. The state relationship matrix, relating the velocity discontinuities and constraints in the solution to the patch point positions and times, is then employed to simultaneously reduce all of the velocity discontinuities present in the trajectory and to satisfy any constraints. The resulting numerical solutions retain the general characteristics designed using the initial estimate and are fully continuous in position, time, and velocity.

It is concluded that use of the three-step design process results in an accurate, efficient method of constructing multiple-lunar-swingby trajectories that meet the design specifications for the problem. Furthermore, it is hoped that this procedure will prove useful in the determination of other types of solutions in the sun–Earth–moon system, as well as other planetary systems.

Acknowledgments

Portions of this work were supported by Purdue University and the Indiana Space Grant Consortium. The authors would like to thank Brian Barden of Purdue University for numerical data used to generate the libration point orbit transfer example.

References

[1]Wilson, R. S., "A Design Tool for Constructing Multiple Lunar Swingby Trajectories," M.S. Thesis, School of Aeronautics and Astronautics, Purdue Univ., West Lafayette, IN, Dec. 1993.

[2]Wilson, R. S., and Howell, K. C., "A Design Concept for Multiple Lunar Swingby Trajectories," AIAA Paper 94-3718, Aug. 1994.

[3]Farquhar, R. W., and Dunham, D. W., "A New Trajectory Concept for Exploring the Earth's Geomagnetic Tail," *Journal of Guidance and Control*, Vol. 4, No. 2, 1981, pp. 192–196.

[4]Marsh, S. M., and Howell, K. C., "Double Lunar Swingby Trajectory Design," *Proceedings of the AIAA/AAS Astrodynamics Conference*, AIAA, Washington, DC, 1988, pp. 554–562.

[5]Howell, K. C., Barden, B. T., and Lo, M. W., "Application of Dynamical Systems Theory to Trajectory Design for a Libration Point Mission," *Journal of the Astronautical Sciences*, Vol. 45, No. 2, 1997, pp. 161–178.

[6]Ishii, N., and Matsuo, H., "Design Procedure of Accurate Orbits in a Multi-Body Frame with a Multiple Swingby," American Astronautical Society, AAS Paper 93-655, Aug. 1993.

[7]Spencer, D. A., "Multiple Lunar Encounter Trajectory Design Using a Multi-Conic Approach," M.S. Thesis, School of Aeronautics and Astronautics, Purdue Univ., West Lafayette, IN, Dec. 1991.

[8]Goodyear, W. H., "A General Method for the Computation of Cartesian Coordinates and Partial Derivatives of the Two-Body Problem," NASA CR-522, Sept. 1966.

[9]Howell, K. C., and Marsh, S. M., "A General Timing Condition for Consecutive Collision Orbits in the Limiting Case $\mu = 0$ of the Elliptic Restricted Problem," *Celestial Mechanics*, Vol. 52, No. 2, 1991, pp. 167–194.

[10]Marsh, S. M., "Sun-Synchronous Trajectory Design Using Consecutive Lunar Gravity Assists," M.S. Thesis, School of Aeronautics and Astronautics, Purdue Univ., West Lafayette, IN, May 1988.

[11]Wilson, S. W., "A Pseudostate Theory for the Approximation of Three-Body Trajectories," AIAA Paper 70-1061, Aug. 1970.

[12]Byrnes, D. V., and Hooper, H. L., "Multi-Conic: A Fast and Accurate Method of Computing Space Flight Trajectories," AIAA Paper 70-1062, Aug. 1970.

[13]Byrnes, D. V., "Application of the Pseudostate Theory to the Three-Body Lambert Problem," *Journal of the Astronautical Sciences*, Vol. 37, July–Sept. 1989, pp. 221–232.

[14]D'Amario, L. A., Byrnes, D. V., Sackett, L. L., and Stanford, R. H., "Optimization of Multiple Flyby Trajectories," American Astronautical Society, AAS Paper 79-162, June 1979.

F. H. Lutze Jr.
Associate Editor